

# Microwave dielectric properties and microstructures of $\text{Nb}_2\text{O}_5\text{-Zn}_{0.95}\text{Mg}_{0.05}\text{TiO}_3 + 0.25\text{TiO}_2$ ceramics with $\text{Bi}_2\text{O}_3$ addition

Ying-Chieh Lee<sup>\*</sup>, Cheng-Su Chiang, Yen-Lin Huang

Department of Material Engineering, National Pingtung University of Science & Technology, Pingtung, Taiwan, ROC

Received 20 May 2009; received in revised form 15 September 2009; accepted 28 September 2009

Available online 24 October 2009

## Abstract

The effects of  $\text{Bi}_2\text{O}_3$  addition on the microwave dielectric properties and the microstructures of  $\text{Nb}_2\text{O}_5\text{-Zn}_{0.95}\text{Mg}_{0.05}\text{TiO}_3 + 0.25\text{TiO}_2$  (Nb-ZMT') ceramics prepared by conventional solid-state routes have been investigated. The results of X-ray diffraction (XRD) indicate the presence of four crystalline phases,  $\text{ZnTiO}_3$ ,  $\text{TiO}_2$ ,  $\text{Bi}_2\text{Ti}_2\text{O}_7$ , and  $(\text{Bi}_{1.5}\text{Zn}_{0.5})(\text{Ti}_{1.5}\text{Nb}_{0.5})\text{O}_7$  in the sintered ceramics, depending upon the amount of  $\text{Bi}_2\text{O}_3$  addition. In addition, in order to confirm the existence of  $(\text{Bi}_{1.5}\text{Zn}_{0.5})(\text{Ti}_{1.5}\text{Nb}_{0.5})\text{O}_7$  phase in the samples, the microstructure of Nb-ZMT' ceramic with 5 wt.%  $\text{Bi}_2\text{O}_3$  addition was analyzed by using a transmission electron micrograph. The dielectric constant of Nb-ZMT' samples was higher than ZMT' ceramics. The Nb-ZMT' ceramic with 5 wt.%  $\text{Bi}_2\text{O}_3$  addition exhibits the optimum dielectric properties:  $Q \times f = 12,000 \text{ GHz}$ ,  $\epsilon_r = 30$ , and  $\tau_f = -12 \text{ ppm/}^\circ\text{C}$ . Unlike the ZMT' ceramic sintered at  $900^\circ\text{C}$ , the Nb-ZMT' ceramics show higher  $Q$  value and dielectric constant. Moreover, there is no  $\text{Zn}_2\text{TiO}_4$  existence at  $960^\circ\text{C}$  sintering. To understand the co-sinterability between silver electrodes and the Nb-ZMT' dielectrics, the multilayer samples are prepared by multilayer thick film processing. The co-sinterability ( $900^\circ\text{C}$ ) between silver electrode and Nb-ZMT' dielectric are well compatible, because there are no cracks, delaminations, and deformations in multilayer specimens.

© 2009 Elsevier Ltd. All rights reserved.

**Keywords:** Nb-ZMT' ( $\text{Nb}_2\text{O}_5\text{-Zn}_{0.95}\text{Mg}_{0.05}\text{TiO}_3 + 0.25\text{TiO}_2$ ); Dielectric resonator; Quality factor;  $\text{Bi}_2\text{O}_3$ ; Microwave ceramic; LTCC

## 1. Introduction

Recently, the development of commercial wireless technologies has made rapid progress because of the improved characteristics of dielectric resonators in microwave ranges. This rapid development of the wireless communication implies to design new ceramics sinterable at low temperature, e.g., at around  $900^\circ\text{C}$  and exhibiting good dielectric properties. This low sintering temperature is of primary importance to produce silver co-sintering devices such as silver based multilayer ceramic capacitors or hybrid circuits.<sup>1–3</sup> The required specifications in term of dielectrics properties are a high dielectric constant ( $\epsilon_r > 20$ ), a high quality factor ( $Q > 10,000$ ) which corresponds to a low dielectric loss ( $\tan \delta = 1/Q$ ) and a temperature coefficient of the permittivity close to zero  $\text{ppm/}^\circ\text{C}$ . However, the sintering temperature of conventional dielectric ceramics used for microwave resonators, filters, and duplexers of portable

phones usually ranges from  $1200$  to  $1500^\circ\text{C}$ .<sup>2,4</sup> Therefore, these dielectric ceramics are not suitable for use in the conductors that have low melting temperatures such as silver ( $961^\circ\text{C}$ ) and copper ( $1064^\circ\text{C}$ ). The development of materials began with the search for a suitable low-firing-temperature dielectric, followed by the modification of the electrical characteristics to meet the above requirements for the specified applications.

There are three compound phases present in the  $\text{ZnO-TiO}_2$  phase diagram:  $\text{Zn}_2\text{TiO}_4$  (cubic),  $\text{ZnTiO}_3$  (hexagonal), and  $\text{Zn}_2\text{Ti}_3\text{O}_8$  (cubic), which is a low-temperature form of  $\text{ZnTiO}_3$  that exists below  $820^\circ\text{C}$ .<sup>5,6</sup> It has been reported that the zinc titanates ( $\text{ZnTiO}_3$ ) can be sintered at  $1100^\circ\text{C}$  without sintering aids.<sup>7</sup> However, if a sintering aid is added, it can be fired at temperatures lower than  $900^\circ\text{C}$ .<sup>7–9</sup> This material has a permittivity ( $\epsilon_r$ ) of 19, a  $Q$  value of 3000 at 10 GHz, and a temperature coefficient ( $\tau_f$ ) of  $-55 \text{ ppm/}^\circ\text{C}$ . Kim et al.<sup>9</sup> studied the  $\text{ZnTiO}_3\text{-}x\text{TiO}_2$  system, where  $x = 0\text{--}0.5$ ; the optimum microwave dielectric properties were obtained to be  $\tau_f = -20 \text{ ppm/}^\circ\text{C}$ ,  $\epsilon_r = 27.5$ , and  $Q \times f = 14,000 \text{ GHz}$  for  $x = 0.25$  and sintered at  $925^\circ\text{C}$ . Nevertheless, the pure  $\text{ZnTiO}_3$  phase is not easily obtained because the compound decomposes to

<sup>\*</sup> Corresponding author. Tel.: +886 87703202; fax: +886 87740552.  
E-mail address: [YCLee@mail.npust.edu.tw](mailto:YCLee@mail.npust.edu.tw) (Y.-C. Lee).

$\text{Zn}_2\text{TiO}_4$  and  $\text{TiO}_2$  at high temperatures.<sup>10</sup> Kim et al.<sup>8</sup> also studied zinc titanate with a small amount of magnesium addition, and reported that the  $(\text{Zn}_{1-x}\text{Mg}_x)\text{TiO}_3$  phase was stable at a much higher temperature, the microwave dielectric properties of which were  $\tau_f = -90 \text{ ppm}/^\circ\text{C}$ ,  $\varepsilon_r = 21$ , and  $Q \times f = 40,000$  at  $x = 0.05$  sintered at  $900^\circ\text{C}$ .

In the previous study,<sup>11</sup> the microstructure and dielectric properties of the  $\text{Bi}_2\text{O}_3$  additive in  $\text{Zn}_{0.95}\text{Mg}_{0.05}\text{TiO}_3 + 0.25\text{TiO}_2$  with 1 wt.%  $3\text{ZnO}-\text{B}_2\text{O}_3$  ceramics have been investigated. It was found that 5 wt.%  $\text{Bi}_2\text{O}_3$  addition can significantly suppress spinel  $\text{Zn}_2\text{TiO}_4$  phase formation in the ZMT' ceramics, but the microwave dielectric properties become worse due to low  $Q$  value ( $<600$ ). Although, the permittivity still was kept at  $\sim 24$ . The main purpose of incorporating 0.8 mol.%  $\text{Nb}_2\text{O}_5$  additive in  $\text{Zn}_{0.95}\text{Mg}_{0.05}\text{TiO}_3 + 0.25\text{TiO}_2$  ceramics is to improve the microwave dielectric properties of sintered samples at lower temperatures, to obtain a homogeneous microstructure, and to suppress spinel  $\text{Zn}_2\text{TiO}_4$  phase formation in this study. In addition, the multilayer specimens were fabricated by multilayer thick film processing. The co-sinterability between silver electrodes and the Nb-ZMT' dielectrics is also studied in this experiment.

## 2. Experimental procedures

### 2.1. Preparation of ZMT' and Nb-ZMT' ceramics

Samples of ZMT' were synthesized by conventional solid-state methods from individual high-purity oxide powders: ZnO (Hayashi Chemical Industry, Japan,  $>99.9\%$ ),  $\text{TiO}_2$  (Janssen Chemica, Japan,  $>99.9\%$ ), MgO (Showa Chemicals Inc., Japan,  $>99.9\%$ ). The starting materials were ZnO, MgO and  $\text{TiO}_2$  powders. They were mixed and ground in deionized water with 2 mm zirconia beads for 24 h, until the mean particle size (D50) was approximately  $0.35 \mu\text{m}$ . The optimum composition of ZMT' determined in previous studies is  $\text{Zn}_{0.95}\text{Mg}_{0.05}\text{TiO}_2 + 0.25\text{TiO}_2$  (ZMT'),<sup>8,9</sup> which is adopted as the reference composition. The powders were calcined in air at  $900^\circ\text{C}$  for 5 h after ball milling.  $\text{Nb}_2\text{O}_5$  was added and fixed at 0.8 mol.%.  $\text{Bi}_2\text{O}_3$  glass was chosen as sintering aids, and it was added in the amounts of 1, 3, 5 and 10 wt.%, respectively. Then the calcined powders were milled again for 6 h. After grinding, the mean particle size was measured to be about  $0.5 \mu\text{m}$ . After drying, the powders were pressed uniaxially into pellets in a steel die. Sintering of these pellets were carried out at 900, 920 and  $940^\circ\text{C}$ , respectively.

### 2.2. Fabrication of multilayered Nb-ZMT' capacitors

In this experiment, MLCC consists of 10 active layers with an overall size of  $2.0 \text{ mm} \times 1.25 \text{ mm} \times 0.6 \text{ mm}$  and a distance of  $17 \mu\text{m}$  between the internal electrodes. The dielectric in the MLCC is a ceramic material based on the Nb-ZMT' compound. The Nb-ZMT' powders were mixed with a resin (polyvinyl butyral), a plasticizer (butyl benzyl phthalate) and a solvent (toluene and ethanol). The resultant slurry was tape casted to a

green sheet with  $30 \mu\text{m}$  thickness using the doctor-blade method. Ag pastes were printed as an inner electrode onto the green sheet. These printed sheets were stacked, pressed at  $60^\circ\text{C}$  under a pressure of  $5.2 \times 10^7 \text{ Pa}$ , and cut into chips. The laminated green chip was sintered from 860 to  $920^\circ\text{C}$  for 2 h after binder burnout ( $320^\circ\text{C}$ ), and then heat treated at  $760^\circ\text{C}$  for Ag end-termination.

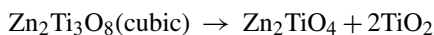
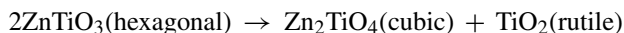
### 2.3. Characteristics analysis

The crystalline phases of the sintered ceramics were identified by X-ray diffraction pattern analysis (XRD, Bruker D8A) using  $\text{Cu-K}\alpha$  radiation for  $2\theta$  from  $20$  to  $60^\circ$ . The diffraction spectra were collected at a scan rate of  $2.5^\circ/\text{min}$ . Microstructural observation of the sintered ceramics was performed by scanning electron microscopy (SEM, Jeol. JEL-6400, Japan) equipped with energy-dispersive spectroscopy (EDS). The bulk density of the sintered pellets was measured by the Archimedes method. The particle size was measured using a particle size analyzer (Malvern, Mastersizer 2000, UK). The dielectric characteristics at microwave frequencies ( $7.25\text{--}9.31 \text{ GHz}$ ) were measured by the Hakki-Coleman dielectric resonator method, where a cylindrically shaped specimen was positioned between two plates.<sup>12</sup> An HP8719C network analyzer was used to measure the microwave property. The dielectric properties were calculated from the frequency of the  $\text{TE}_{011}$  resonant mode. For convenience, the  $Q \times f$  factor was used to evaluate the loss quality, where  $f$  is the resonant frequency.

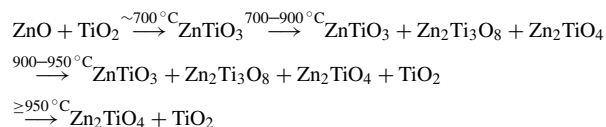
## 3. Results and discussion

### 3.1. Effect of $\text{Bi}_2\text{O}_3$ addition on phase evolution and microstructure of the ceramics

The hexagonal  $\text{ZnTiO}_3$  phase remains stable at temperatures below  $945^\circ\text{C}$  and then decomposes to the cubic  $\text{Zn}_2\text{TiO}_4$  and  $\text{TiO}_2$  phases at  $945^\circ\text{C}$ , as indicated in the phase diagram of  $\text{ZnO}-\text{TiO}_2$ .<sup>5</sup> The  $\text{Zn}_2\text{Ti}_3\text{O}_8$  phase, known as the low-temperature form of the  $\text{ZnTiO}_3$  phase, exists at temperatures between 900 and  $925^\circ\text{C}$ . In fact, the decomposition of  $\text{ZnTiO}_3$  and  $\text{Zn}_2\text{Ti}_3\text{O}_8$  phases starts at  $\sim 900^\circ\text{C}$  and completes at  $\sim 950^\circ\text{C}$ . The decomposition reactions of the two compounds at  $\sim 950^\circ\text{C}$  can be describe as follows.



In reality, small amounts of the  $\text{Zn}_2\text{TiO}_4$  phase were also detected at  $900^\circ\text{C}$  as a counterpart of  $\text{Zn}_2\text{Ti}_3\text{O}_8$  to satisfy the stoichiometry. Therefore, the formation and transformation reactions of  $\text{ZnTiO}_3$  can be summarized as follows.



These results indicate that the cubic  $\text{Zn}_2\text{Ti}_3\text{O}_8$  phase is an intermediate phase of the  $\text{ZnO}-\text{TiO}_2$  system that exists at

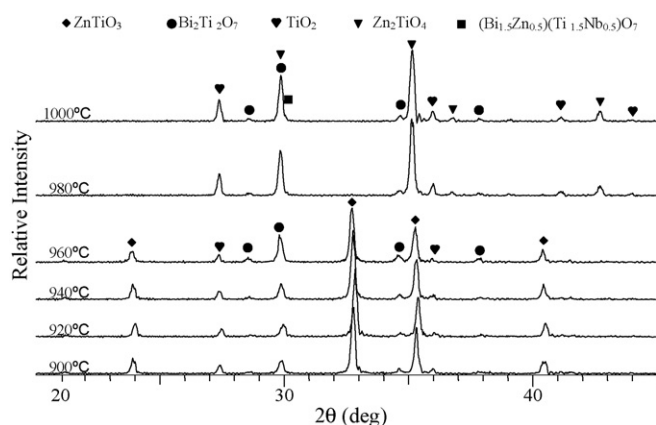


Fig. 1. X-ray diffraction (XRD) spectra of Nb-ZMT' ceramics with 5 wt.%  $\text{Bi}_2\text{O}_3$  sintered at (a) 900 °C, (b) 920 °C, (c) 940 °C, (d) 960 °C, (e) 980 °C, and (f) 1000 °C.

700–950 °C, rather than a low-temperature form of  $\text{ZnTiO}_3$ .<sup>6,8</sup>

Fig. 1 shows the XRD results for Nb-ZMT' with 5 wt.%  $\text{Bi}_2\text{O}_3$  addition sintered at temperatures ranging from 900 to 1000 °C. It is interesting to note that no cubic  $\text{Zn}_2\text{TiO}_4$  phase is present in the Nb-ZMT' ceramic with 5 wt.%  $\text{Bi}_2\text{O}_3$  addition, even at a temperature as high as 960 °C. This is contradicted by the phase diagram, which indicates that the  $\text{ZnTiO}_3$  ceramic would decompose at 945 °C. This result is the same as previous study,<sup>11</sup>  $\text{Bi}_2\text{O}_3$  addition can be inhibited  $\text{Zn}_2\text{TiO}_4$  formation in ZMT' ceramics at sintered temperatures of up to 960 °C. Also from our previous study,<sup>13</sup> it is known that the  $\text{Zn}_2\text{TiO}_4$  phase was formed in ZMT' ceramics with 1 wt.%  $3\text{ZnO}-\text{Bi}_2\text{O}_3$  addition sintered at 920 °C. In other words, it can be concluded that the addition of  $\text{Bi}_2\text{O}_3$  can suppress the formation of the  $\text{Zn}_2\text{TiO}_4$  phase in the Nb-ZMT' ceramics. Fig. 2 shows the XRD results for Nb-ZMT' ceramics sintered at 900 °C with different amounts of  $\text{Bi}_2\text{O}_3$ . For the undoped Nb-ZMT' ceramics sintered at 900 °C, as shown in Fig. 2(a), it can be observed that the ceramic contains two well-characterized phases, namely  $\text{TiO}_2$  and  $\text{ZnTiO}_3$ .<sup>14</sup> For Nb-ZMT' ceramics with 3, 5 and 10 wt.%  $\text{Bi}_2\text{O}_3$  additions sintered at 900 °C, as shown in Fig. 2(c)–(e), respectively, it is found that the major

crystalline phases are the same as those of the undoped Nb-ZMT' ceramics, along with two extra-phases identified to be  $\text{Bi}_2\text{Ti}_2\text{O}_7$  and  $(\text{Bi}_{1.5}\text{Zn}_{0.5})(\text{Ti}_{1.5}\text{Nb}_{0.5})\text{O}_7$ . When  $\text{Bi}_2\text{O}_3$  and  $\text{Nb}_2\text{O}_5$  are doped into ZMT' ceramics,  $\text{Nb}^{5+}$  obviously exhibit a preference for the Ti-sites, since the ionic radius of  $\text{Ti}^{4+}$  ( $r=0.605$  Å) is close to that of  $\text{Nb}^{5+}$  ( $r=0.64$  Å), and  $\text{Bi}^{3+}$  substitute a preference for the Zn-sites, because the ionic radius of  $\text{Zn}^{2+}$  ( $r=0.74$  Å) is close to that of  $\text{Bi}^{3+}$  ( $r=0.81$  Å). It can be assumed that small amount of  $(\text{Bi}_{1.5}\text{Zn}_{0.5})(\text{Ti}_{1.5}\text{Nb}_{0.5})\text{O}_7$  is formed based on element ionic radius, because the XRD analysis revealed that the phase structures of substituted sample has a  $\text{Bi}_2\text{Ti}_2\text{O}_7$  phase (Fig. 2). That means  $\text{Nb}^{5+}$  partly substituting for  $\text{Ti}^{4+}$  at B site and  $\text{Bi}^{3+}$  partly substituting for  $\text{Zn}^{2+}$  at A site result a relatively stable substitutional solid solution  $(\text{Bi}_{1.5}\text{Zn}_{0.5})(\text{Ti}_{1.5}\text{Nb}_{0.5})\text{O}_7$ . It is not easy to identify the phases between  $\text{Bi}_2\text{Ti}_2\text{O}_7$  and  $(\text{Bi}_{1.5}\text{Zn}_{0.5})(\text{Ti}_{1.5}\text{Nb}_{0.5})\text{O}_7$  compounds, since the angles and intensities of peak are almost the same between them from XRD data. However, the amount of  $(\text{Bi}_{1.5}\text{Zn}_{0.5})(\text{Ti}_{1.5}\text{Nb}_{0.5})\text{O}_7$  phase formed in ZMT' ceramics is less than  $\text{Bi}_2\text{Ti}_2\text{O}_7$  phase due to  $\text{Nb}_2\text{O}_5$  doped is only 0.8 mol.% and the Nb has solubility limit. The  $(\text{Bi}_{1.5}\text{Zn}_{0.5})(\text{Ti}_{1.5}\text{Nb}_{0.5})\text{O}_7$  phase was further analyzed by transmission electron micrograph (TEM).

Fig. 3 shows the XRD results of the sintered ceramics having the composition of Nb-ZMT' with different amounts of  $\text{Bi}_2\text{O}_3$ . We separated two groups for discussion, one is Nb-ZMT' with different amounts of  $\text{Bi}_2\text{O}_3$  sintered at 920 °C (Fig. 3(a)–(c)), the other one is Nb-ZMT' with different amounts of  $\text{Bi}_2\text{O}_3$  sintered at 940 °C (Fig. 3(d)–(f)). For the composition of Nb-ZMT' ceramics with 1 wt.%  $\text{Bi}_2\text{O}_3$  addition sintered at 920 °C, as shown in Fig. 3(a), it can be observed that the ceramic contains  $\text{TiO}_2$ ,  $\text{ZnTiO}_3$  and  $\text{Bi}_2\text{Ti}_2\text{O}_7$  phases. For the composition of Nb-ZMT' ceramics with 3 and 5 wt.%  $\text{Bi}_2\text{O}_3$  additions, as shown in Fig. 3(b) and (c), respectively, it is found that the major crystalline phases are the same as those of the Nb-ZMT' ceramics with 1 wt.%  $\text{Bi}_2\text{O}_3$  additions, without extra-phases are identified. When the sintering temperature rises from 920 to 940 °C, the microstructure of the ceramics is change a lot. For the composition of Nb-ZMT' ceramics with 1 wt.%  $\text{Bi}_2\text{O}_3$  addi-

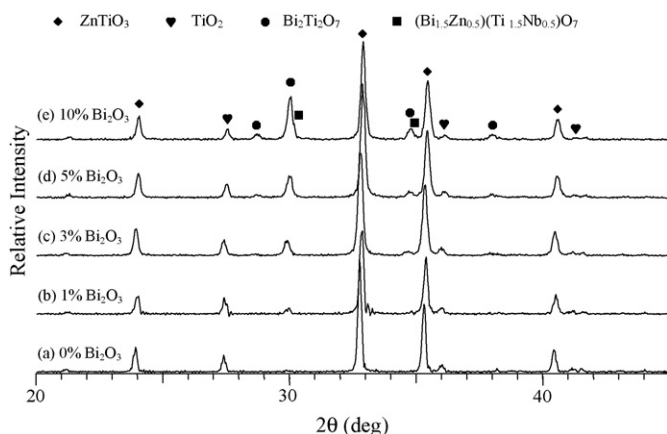


Fig. 2. X-ray diffraction (XRD) spectra of Nb-ZMT' ceramics sintered at 900 °C with dopant (a) 0 wt.%, (b) 1 wt.%, (c) 3 wt.%, (d) 5 wt.% and (e) 10 wt.%  $\text{Bi}_2\text{O}_3$ .

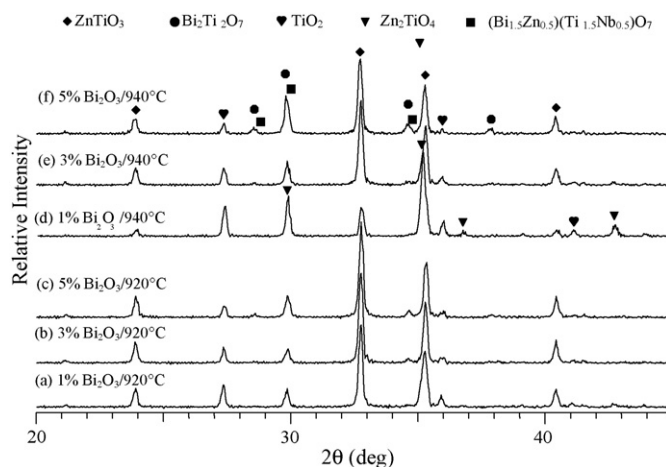


Fig. 3. X-ray diffraction (XRD) spectra of Nb-ZMT' ceramics with different  $\text{Bi}_2\text{O}_3$  contents/sintering temperature: (a) 1%/920 °C, (b) 1%/940 °C, (c) 3%/920 °C, (d) 3%/940 °C, (e) 5%/920 °C, and (f) 5%/940 °C.



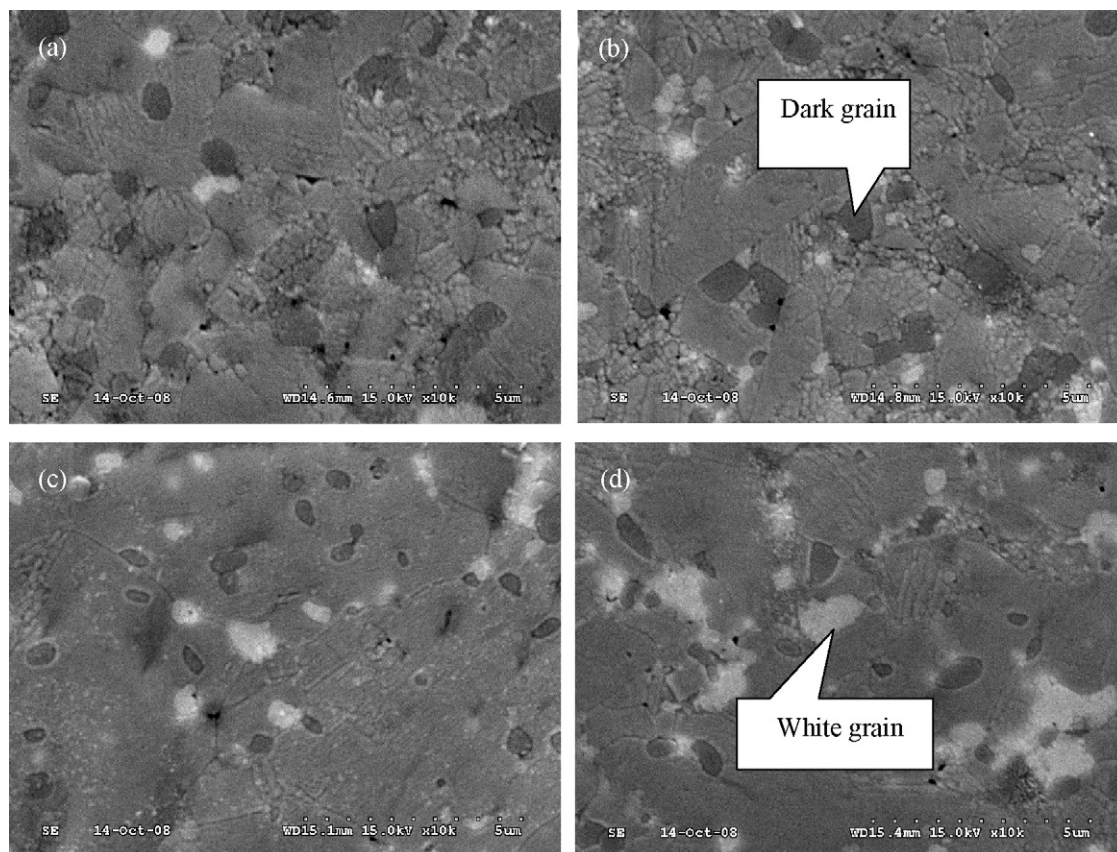


Fig. 4. SEM micrographs of the Nb-ZMT' ceramics sintered at 900 °C with (a) 1 wt.%, (b) 3 wt.%, (c) 5 wt.% and (d) 10 wt.%  $\text{Bi}_2\text{O}_3$ .

tion sintered at 940 °C, as shown in Fig. 3(d), there are contained three phases in the sample, namely  $\text{TiO}_2$ ,  $\text{ZnTiO}_3$  and  $\text{Zn}_2\text{TiO}_4$ . When the same heat treatments were applied in Nb-ZMT' ceramics with 5 wt.%  $\text{Bi}_2\text{O}_3$  addition (Fig. 3(f)), the microstructure of the ceramics mainly consisted of  $\text{TiO}_2$ ,  $\text{ZnTiO}_3$  and  $\text{Bi}_2\text{Ti}_2\text{O}_7$ . This result indicates that the  $\text{Bi}_2\text{O}_3$  dopant content and sintering temperature play an important role, which suppress the formation of the  $\text{Zn}_2\text{TiO}_4$  phase in the Nb-ZMT' ceramics.

Fig. 4 shows SEM micrographs of the Nb-ZMT' ceramics sintered at 900 °C with 1, 3, 5, and 10 wt.%  $\text{Bi}_2\text{O}_3$  addition. It seems that the microstructures are closely correlated to the  $\text{Bi}_2\text{O}_3$  content. The gray, similar rectangular grains are  $\text{ZnTiO}_3$  phases, the dark grains are rutile phases ( $\text{TiO}_2$ ) [9], and the white grains are second phases ( $\text{Bi}_2\text{Ti}_2\text{O}_7$ ). However, the microstructure of the sintered ceramics shows a slight change, that is, a new second phase is increased significantly with the increasing of  $\text{Bi}_2\text{O}_3$  content, as shown in Fig. 3(c) and (d), for those samples which contain 5 and 10 wt.%  $\text{Bi}_2\text{O}_3$ , respectively. The volume of second phase grain is ~6% and ~15% for sample with 5 and 10 wt.%  $\text{Bi}_2\text{O}_3$  addition, respectively. The second phase was further analyzed by TEM energy-dispersive-spectroscopy, and the results for Nb-ZMT' ceramics with 5 wt.%  $\text{Bi}_2\text{O}_3$  addition sintered at 900 °C for 2 h are shown in Fig. 5. TEM-EDX and TEM-electron diffraction were used to provide more detailed information on these intergranular phases in the samples. However, according to XRD identification, there are four phases in the BST with 5 wt.%  $\text{Bi}_2\text{O}_3$  addition, these phases are included

$\text{ZnTiO}_3$ ,  $(\text{Bi}_{1.5}\text{Zn}_{0.5})(\text{Ti}_{1.5}\text{Nb}_{0.5})\text{O}_7$ ,  $\text{Bi}_2\text{Ti}_2\text{O}_7$ , and  $\text{TiO}_2$ . The EDX results of part A (Fig. 5(b)), showed only Zn, Ti and O in the matrix; no Nb and Bi were detected. For this matrix phase A, an electron diffraction pattern was done as shown in Fig. 5(f), the result indicates this matrix phase should be a  $\text{ZnTiO}_3$ . The EDX results of part B, it did provide an indication of Nb in phase B (Fig. 5(c)). Therefore, phase B, which XRD data had suggested to be  $(\text{Bi}_{1.5}\text{Zn}_{0.5})(\text{Ti}_{1.5}\text{Nb}_{0.5})\text{O}_7$ . This result can be supported by electron diffraction pattern analyzing as shown in Fig. 5(g). For the EDX data of part C and D (Fig. 5(d)–(e)), the results indicate that the compounds should be  $\text{TiO}_2$ , and  $\text{Bi}_2\text{Ti}_2\text{O}_7$ , respectively. The phase D analyzed by EDX contained Bi, Ti and O with low levels of Nb and Zn, Fig. 5(e). Therefore, this phase was the Nb and Zn-containing phase D, suggested by XRD to be  $\text{Bi}_2\text{Ti}_2\text{O}_7$ . TEM-EDX, as with phase D, indicated a low level of Nb substituted to Ti and Zn replaced to Bi.

### 3.2. Effect of $\text{Bi}_2\text{O}_3$ addition on microwave dielectric properties of the ceramics

The dielectric constant of the ceramics was measured, and the results are shown in Fig. 6(a). The  $\epsilon_r$  value of Nb-ZMT' ceramics is significantly related to the  $\text{Bi}_2\text{O}_3$  content, e.g., the dielectric constants of the ceramic are 25.1, 27.8, 30.2 and 31.6 for  $\text{Bi}_2\text{O}_3$  content at 1, 3, 5 and 10 wt.%, respectively. In addition, the dielectric constants of the ZMT' ceramics (undoped  $\text{Nb}_2\text{O}_5$ ) with different amounts of  $\text{Bi}_2\text{O}_3$  addition are kept at ~24. Unlike

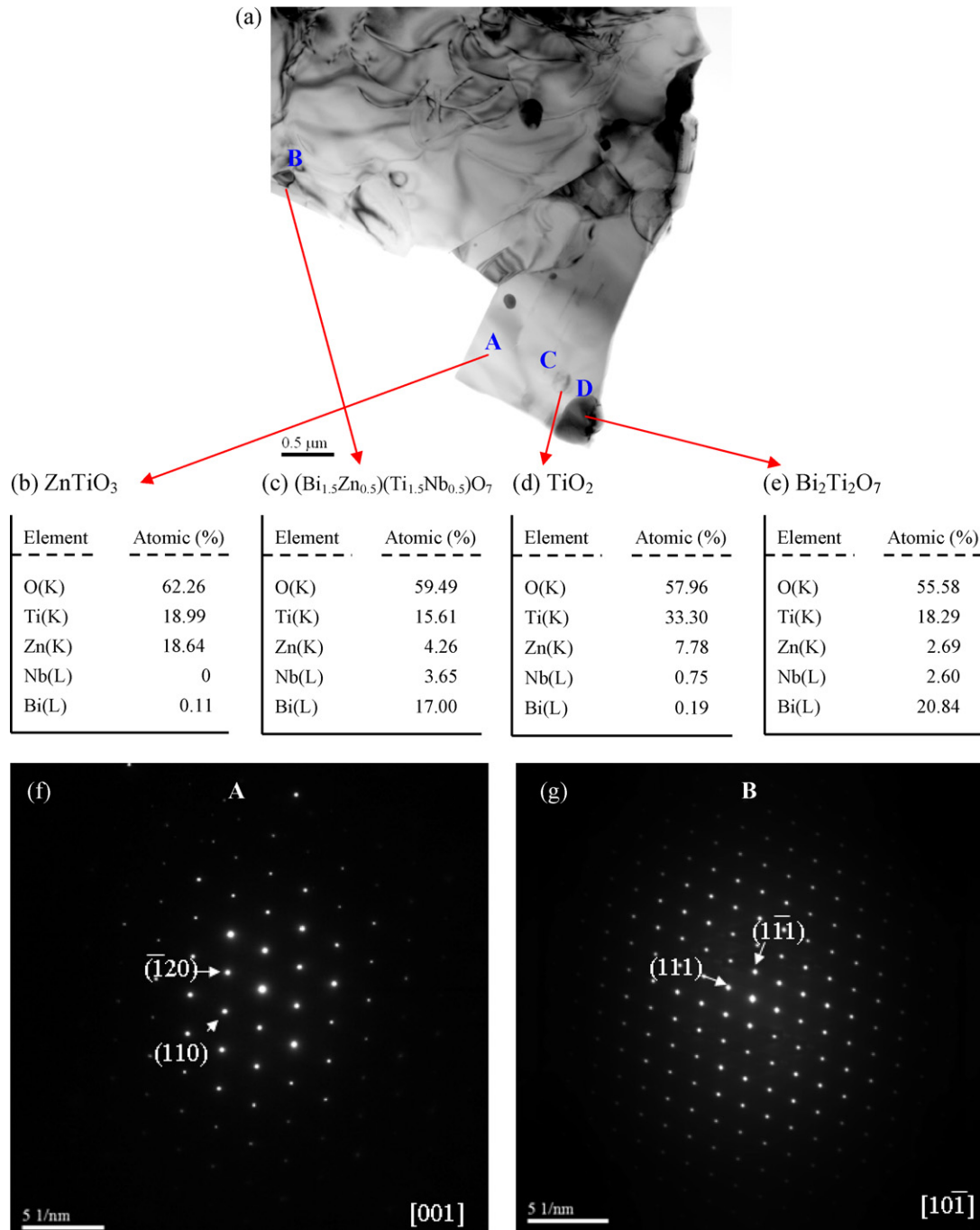


Fig. 5. TEM analysis for the specimen with 5 wt.%  $\text{Bi}_2\text{O}_3$  addition sintered at  $900^\circ\text{C}$  (a) micrograph, (b) EDX data of A part, (c) EDX data of B part, (d) EDX data of C part, (e) EDX data of D part, (f) diffraction pattern of A part and (g) diffraction pattern of B part.

the Nb-ZMT' ceramics with  $\text{Bi}_2\text{O}_3$  addition, the ZMT' ceramics with increasing amounts of  $\text{Bi}_2\text{O}_3$  show slightly variation of dielectric constant. In a previous study,<sup>11</sup> we have investigated the microwave dielectric properties of the ZMT' ceramics with different amounts of  $\text{Bi}_2\text{O}_3$  addition. A comparison between the ceramics with and without  $\text{Nb}_2\text{O}_5$  dopant on the microstructure of the ceramics will be described briefly below. The XRD results show that both of the sintered ceramics with  $\text{Bi}_2\text{O}_3$  addition contain the three crystalline phases,  $\text{ZnTiO}_3$ ,  $\text{TiO}_2$ , and  $\text{Bi}_2\text{Ti}_2\text{O}_7$ . Nevertheless, dopant of  $\text{Nb}_2\text{O}_5$  in the ZMT' ceramics also produces the  $(\text{Bi}_{1.5}\text{Zn}_{0.5})(\text{Ti}_{1.5}\text{Nb}_{0.5})\text{O}_7$  phase, this is

$\text{A}_2\text{B}_2\text{O}_7$  cubic pyrochlores phase. As we known,<sup>15</sup> pyrochlore-type oxides with the general formula  $(\text{Bi}_{1.5}\text{Zn}_{0.5})(\text{Ti}_{1.5}\text{Nb}_{0.5})\text{O}_7$  (BZTN) have been attracting a lot of attention because of their excellent dielectric constant and low firing temperature. BZTN ceramic is one of the most promising materials due to its stability and excellent dielectric properties ( $\epsilon_r \sim 200$  and  $\tan \delta = 0.01\%$  at 1 MHz). Therefore, the existence of a small amount of cubic pyrochlores phase can increase the dielectric constant of the ceramic because the dielectric constant of BZTN is much higher than that of the hexagonal  $\text{ZnTiO}_3$  phase,  $\epsilon_r = 19$ .<sup>9</sup> It is therefore believed that the higher dielectric constant is related to the

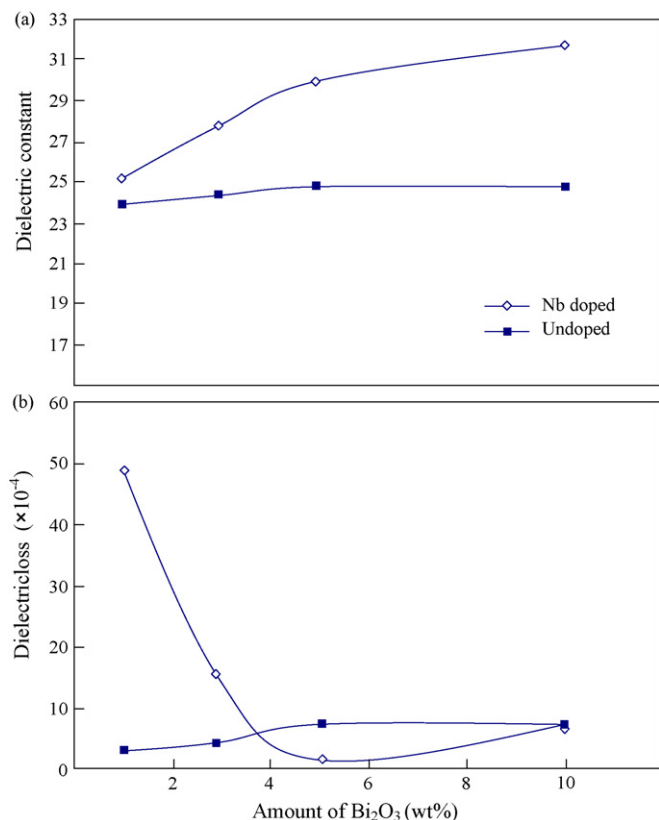


Fig. 6. The dielectric properties of the Nb-ZMT' ceramics sintered at  $900^\circ\text{C}$  as a function of the amount of  $\text{Bi}_2\text{O}_3$  addition, (a) dielectric constants and (b) dielectric loss.

pyrochlores phase evolution when the  $\text{Bi}_2\text{O}_3$  is added in Nb-ZMT' ceramics. The dielectric loss of the ceramics as a function of  $\text{Bi}_2\text{O}_3$  amount is shown in Fig. 6(b). The  $\tan \delta$  value of Nb-ZMT' ceramics is also deeply related to the  $\text{Bi}_2\text{O}_3$  content, and minimum  $\tan \delta$  (0.02%) is obtained at 5 wt.%  $\text{Bi}_2\text{O}_3$  addition. On the other hand, the dielectric loss of the ZMT' ceramics is below 0.1% for the samples with different amounts of  $\text{Bi}_2\text{O}_3$ . However, this result suggests that the Nb-ZMT' ceramics with  $\text{Bi}_2\text{O}_3$  addition can have good dielectric properties, which would be accompanied by an increase in the dielectric constant.

The  $\text{ZnTiO}_3$  ceramic is an interesting material with a negative  $\tau_f$  of  $-55 \text{ ppm}/^\circ\text{C}$ ,  $\epsilon_r$  of 19 and a  $Q$  value of 3000 at 10 GHz.<sup>13</sup> Fig. 7 shows the  $Q \times f$  value of the ceramics as a function of the amount of  $\text{Bi}_2\text{O}_3$ . The  $Q \times f$  values of the ZMT' ceramics without  $\text{Bi}_2\text{O}_3$  addition are higher than that in the case of the Nb-ZMT' ceramics. In contrast, the  $Q \times f$  values of the Nb-ZMT' ceramics with  $\text{Bi}_2\text{O}_3$  addition are higher than that in the case of the ZMT' ceramics. The reason for this is attributed to a formation of  $(\text{Bi}_{1.5}\text{Zn}_{0.5})(\text{Ti}_{1.5}\text{Nb}_{0.5})\text{O}_7$  when the  $\text{Bi}_2\text{O}_3$  is added into Nb-ZMT' ceramics. This cubic pyrochlores phase has excellent dielectric properties as we mentioned above. For ZMT' ceramics, when the 1 wt.%  $\text{Bi}_2\text{O}_3$  was added to the ceramics, the  $Q \times f$  value decreased rapidly from 32,000 to 7000. This result is probably due to the formation of the second phase  $\text{Bi}_2\text{Ti}_2\text{O}_7$  from the low-loss hexagonal ilmenite structure and rutile phase, as illustrated in Fig. 2. It is known that the microwave dielectric loss is mainly controlled by the second phases formed or

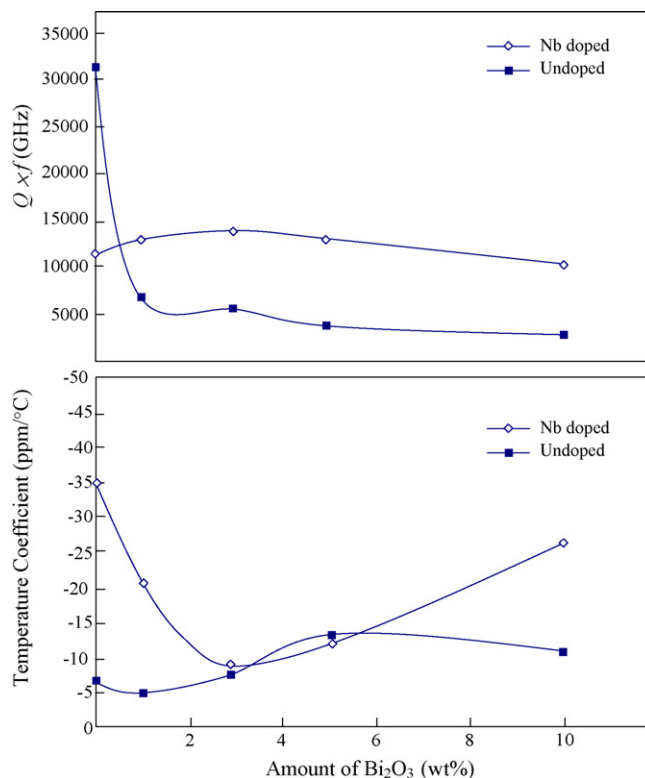


Fig. 7. The  $Q \times f$  values and temperature coefficients of resonant frequency of the Nb-ZMT' ceramics sintered at  $900^\circ\text{C}$  as a function of the amount of added  $\text{Bi}_2\text{O}_3$  addition.

the crystal defects and grain boundaries.<sup>16,17</sup> Nevertheless, from the point of view of practical application, ceramics with a low  $Q \times f$  value are not suitable for high-frequency applications. Moreover, the  $Q \times f$  values of Nb-ZMT' ceramics are slightly increased with  $\text{Bi}_2\text{O}_3$  increasing then slightly decreased at 5 and 10 wt.%  $\text{Bi}_2\text{O}_3$ . Fig. 7 also shows the temperature coefficient of the resonant frequency,  $\tau_f$ , at the maximum  $Q$  value as a function of the amount of  $\text{Bi}_2\text{O}_3$  for samples. The Nb-ZMT' ceramics with 3 wt.%  $\text{Bi}_2\text{O}_3$  addition has a  $\tau_f$  closer to zero than those of other compositions, which is a condition required for microwave device applications. The ZMT' ceramic is known for its temperature-stable characteristic. The  $\tau_f$  values did not change much when  $\text{Bi}_2\text{O}_3$  was added to the ZMT' ceramic. However, the  $\tau_f$  value of the Nb-ZMT' ceramic with 3 wt.%  $\text{Bi}_2\text{O}_3$  addition exhibited the smallest negative value of  $-10 \text{ ppm}/^\circ\text{C}$ .

### 3.3. Dielectric properties and microstructures of the Nb-ZMT' MLCCs

The multilayer specimens were fabricated by tape casting, screen printing, and laminating. A green sheet with  $30 \mu\text{m}$  thickness was obtained by a caster with a doctor blade. Conductor pastes of pure Ag were then printed on it to form the internal electrode. The multilayer specimens were sintered in the range  $860$ – $920^\circ\text{C}$ , and then heat treated at  $760^\circ\text{C}$  for Ag end-termination. Fig. 8 shows scanning electron microscopic pictures for Nb-ZMT' multilayer ceramic capacitors (MLCC) with pure silver electrodes sintered at  $900^\circ\text{C}$ . It is found there are no flaws at the interface. It means that a good physical match



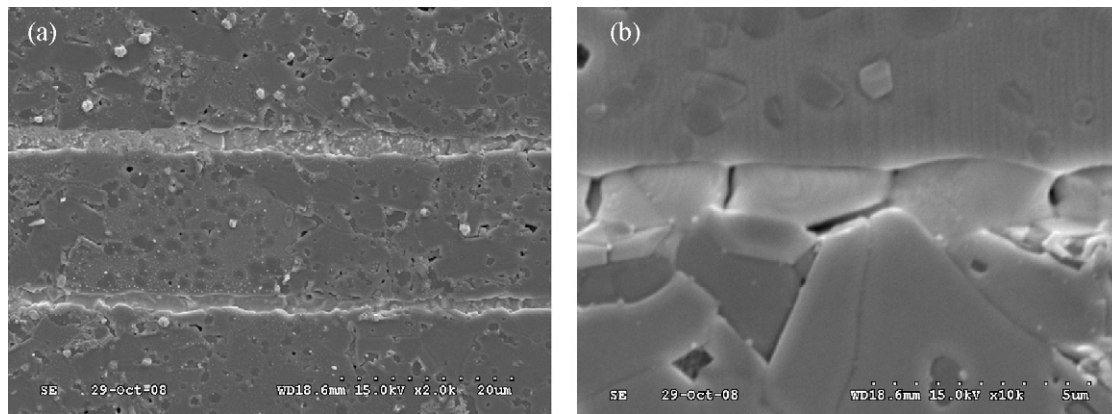


Fig. 8. Scanning electron microscope pictures for Nb-ZMT' multilayer ceramic capacitors with pure silver electrodes sintered at 900 °C, (a) magnification 2000 $\times$ , (b) magnification 10,000 $\times$ .

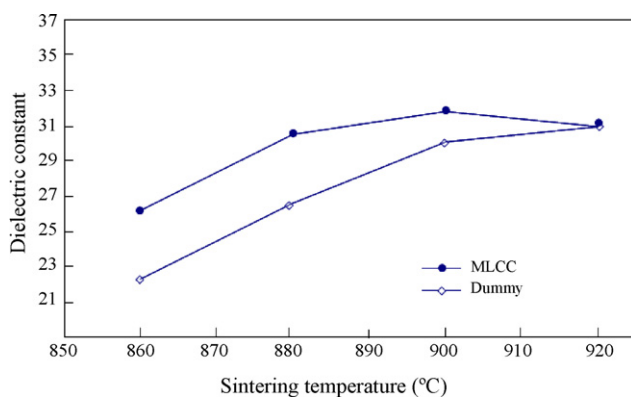


Fig. 9. Dielectric constant of the Nb-ZMT' ceramic and Nb-ZMT' multilayer ceramic capacitors as a function of the sintering temperature.

silver electrode and Nb-ZMT' dielectric. Several papers have pointed out that the cracking, delamination, and deformation of the MLCCs resulting from physical mismatch and sintering shrinkage.<sup>18–20</sup> It is therefore that the Nb-ZMT' ceramic could be compatible for LTCC application. The dielectric constant of the Nb-ZMT' MLCCs as a function of the sintering temperature is shown in Fig. 9. It can be seen that, in general, the dielectric constant of the sintered Nb-ZMT' MLCC increases with the sintering temperature. The decrease of  $\epsilon_r$  can be explained by a reduction of density and the effect of liquid-phase sintering of the Nb-ZMT' MLCCs.<sup>21,22</sup> This trend is the same as Nb-ZMT' ceramic. The multilayer samples have lower  $\epsilon_r$  value after reaching a maximum value at 900 °C. This can be attributed to the low melting point of Ag electrodes with strong shrinkage during sintering at 920 °C. Moreover, it was observed that the dielectric constant of capacitors in the multilayer form is higher than that in the disk form. Two reasons can be given: one is some form of interactions between the thin dielectrics and Ag electrodes are responsible for the higher  $\epsilon_r$ ,<sup>23,24</sup> and the other one is that the low melting point of Ag leads to transient liquid sintering when Ag is transferred to the dielectric layer.<sup>25</sup>

#### 4. Conclusions

The microwave properties and microstructures were affected by the addition of Nb<sub>2</sub>O<sub>5</sub> and Bi<sub>2</sub>O<sub>3</sub> for ZMT' ceramics.

Two kinds of new secondary phases were found in this study; it is believed to be related to Bi<sub>2</sub>O<sub>3</sub>, since it also appeared in specimens that contained  $\geq 3$  wt.% Bi<sub>2</sub>O<sub>3</sub>. A transmission electron microscopy was used to analyze the secondary phases for Nb-ZMT' ceramic with 5 wt.% Bi<sub>2</sub>O<sub>3</sub> addition, both of secondary phases were identified to be Bi<sub>2</sub>Ti<sub>2</sub>O<sub>7</sub> and (Bi<sub>1.5</sub>Zn<sub>0.5</sub>)(Ti<sub>1.5</sub>Nb<sub>0.5</sub>)O<sub>7</sub>. In addition, Bi<sub>2</sub>O<sub>3</sub> addition can be inhibited Zn<sub>2</sub>TiO<sub>4</sub> formation in Nb-ZMT' ceramics at sintered temperatures of up to 960 °C. In this study, Nb-ZMT' ceramics with 5 wt.% Bi<sub>2</sub>O<sub>3</sub> were sintered at 900 °C for 2 h, the dielectric properties were  $Q \times f = 12,000$  GHz,  $\epsilon_r = 30$ , and  $\tau_f = -12$  ppm/°C. On the other hand, the co-sinterability between silver and the Nb-ZMT' dielectric seem to be well compatible, because there are no cracks, delaminations, and deformations in multilayer specimens. It is therefore that the Nb-ZMT' ceramic could be suitable for LTCC application.

#### Acknowledgements

The authors would like to acknowledge the financial support of this study by the National Science Council of Taiwan under Contract No. NSC97-2221-E-020-003.

#### References

- Weng, M. H., Liang, T. J. and Huang, C. L., Lowering of sintering temperature and microwave dielectric properties of BaTi<sub>4</sub>O<sub>9</sub> ceramics prepared by the polymeric precursor method. *J. Eur. Ceram. Soc.*, 2002, **22**, 1693–1698.
- Huang, C. L. and Weng, M. H., Low-fire BiTaO<sub>4</sub> dielectric ceramics for microwave applications. *Mater. Lett.*, 2000, **43**, 32–35.
- Chaouchi, A., Marinel, S., Aliouat, M. and Astorg, S., Low temperature sintering of ZnTiO<sub>3</sub>/TiO<sub>2</sub> based dielectric with controlled temperature coefficient. *J. Eur. Ceram. Soc.*, 2007, **27**, 2561–2566.
- Takada, T., Wang, S. F., Yoshikawa, S., Jang, S. J. and Newnham, R. E., Effects of glass additions on (Zr,Sn)TiO<sub>4</sub> for microwave applications. *J. Am. Ceram. Soc.*, 1994, **77**, 2485–2488.
- Dulin, F. H. and Rase, D. E., Phase equilibria in the system ZnO–TiO<sub>2</sub>. *J. Am. Ceram. Soc.*, 1960, **43**, 125–131.
- Yamaguchi, O., Morimi, M., Kawabata, H. and Shimizu, K., Formation and transformation of ZnTiO<sub>3</sub>. *J. Am. Ceram. Soc.*, 1987, **70**, C97–C98.
- Kim, H. T., Byun, J. D. and Kim, Y. H., Microstructure and microwave dielectric properties of modified zinc titanates (I). *Mater. Res. Bull.*, 1998, **33**, 963–973.

8. Kim, H. T., Nahm, S. and Byun, J. D., Low-fired (Zn,Mg)TiO<sub>3</sub> microwave dielectrics. *J. Am. Ceram. Soc.*, 1999, **82**, 3476–3480.
9. Kim, H. T., Kim, S. H., Nahm, S. and Byun, J. D., Low-temperature sintering and microwave dielectric properties of zinc metatitanate-rutile mixtures using boron. *J. Am. Ceram. Soc.*, 1999, **82**, 3043–3048.
10. Chang, Y. S., Chang, Y. H., Chen, I. G. and Chen, G. J., Synthesis and characterization of zinc titanate doped with magnesium. *Solid State Commun.*, 2003, **128**, 203–208.
11. Lee, Y. C. and Lee, W. H., Effect of glass addition on the microwave dielectric properties of Zn<sub>0.95</sub>Mg<sub>0.05</sub>TiO<sub>3</sub> + 0.25TiO<sub>2</sub> ceramics. *Jpn. J. Appl. Phys.*, 2005, **44**, 1838–1843.
12. Hakki, B. W. and Coleman, P. D., A dielectric resonator method of measuring inductive capacities in the millimeter range. *IRE Trans. Microwave Theory Tech.*, 1960, **8**, 402–410.
13. Lee, Y. C., Lee, W. H. and Shiao, F. T., Microwave dielectric properties of Zn<sub>0.95</sub>Mg<sub>0.05</sub>TiO<sub>3</sub> + 0.25TiO<sub>2</sub> ceramics with 3ZnO–B<sub>2</sub>O<sub>3</sub> addition. *Jpn. J. Appl. Phys.*, 2004, **43**, 7596–7599.
14. Jantunen, H., Rautioaho, R., Unsimaki, A. and Leppavuori, S., Compositions of MgTiO<sub>3</sub>–CaTiO<sub>3</sub> ceramic with two borosilicate glasses for LTCC technology. *J. Eur. Ceram. Soc.*, 2000, **20**, 2331–2336.
15. Liu, Y., Ray, L., Withers, T. R., Welberry, Wang, H. and Du, H., Crystal chemistry on a lattice: the case of BZN and BZN-related pyrochlores. *J. Solid State Chem.*, 2006, **179**, 2141–2149.
16. Yang, C. F., The microwave characteristics of glass–BaTi<sub>4</sub>O<sub>9</sub> ceramics. *Jpn. J. Appl. Phys.*, 1999, **38**, 3576–3579.
17. Hirano, S. I., Hayashi, T. and Hatto, A., Chemical processing microwave characteristics of (Zr,Sn)TiO<sub>4</sub> microwave dielectrics. *J. Am. Ceram. Soc.*, 1991, **74**, 1320–1324.
18. Zuo, R. Z., Li, L. T. and Gui, Z. L., Interfacial development and microstructural imperfection of multilayer ceramic chips with Ag/Pd electrodes. *Ceram. Int.*, 2001, **27**, 889–893.
19. Zuo, R. Z., Li, L. T., Hu, X. B. and Gui, Z. L., Improvement of Ag–Pd alloy electrode by ceramic dopant applied for multilayer electronic ceramic devices. *Mater. Lett.*, 2001, **51**, 504–508.
20. Chen, C. L., Lee, W. H. and Wei, W. C. J., Sintering behavior and interfacial analysis of Ni/Cu electrode with BaTiO<sub>3</sub> particulates. *J. Electroceram.*, 2005, **14**, 25–36.
21. Nakamura, T., Okano, Y. and Miura, S., Interfacial diffusion between Ni–Zn–Cu ferrite and Ag during sintering. *J. Mater. Sci.*, 1998, **33**(4), 1091–1094.
22. Caballero, A. C. and Nieto, E., Ceramic-electrode interaction in PZT and PNN–PZT multilayer piezoelectric ceramics with Ag/Pd 70/30 inner electrode. *J. Mater. Sci.*, 1997, **32**, 3257–3262.
23. Halder, N., Das Sharma, A., Khan, S. K., Sn, A. and Maiti, H. S., Effect of silver addition on the dielectric properties of barium titanate based low temperature processed capacitors. *Mater. Res. Bull.*, 1999, **34**(4), 545–550.
24. Zuo, R. Z., Li, L. T., Gui, Z. L., Hung, T. F. and Xu, Z. K., TEM and EDS investigation of heterogeneous interfaces in cofired multilayer ceramic capacitors. *Mater. Sci. Eng.*, 2002, **B95**, 1–5.
25. Zuo, R. Z., Li, L. T. and Gui, Z. L., Influence of silver migration on dielectric properties and reliability of relaxor based MLCCs. *Ceram. Int.*, 2000, **26**, 673–676.